

Experimental study on flexural behaviours of fresh or aged hollow reinforced concrete girders strengthened by prestressed CFRP plates

Yu Deng^a, Zhen Guo^a, Hexin Zhang^{b,*}, Suchart Limkatanyu^c, Piti Sukontasukkul^d, Terry Y. P. Yuen^e, Simon H.F. Wong^f, Chayanon Hansapinyo^g, Mark Adom-Asamoah^h, Minhe Shen^{a,b}, Longting Huang^b, J.S. Kuangⁱ, Yiqing Zou^{j,*}

^a School of Civil Engineering and Architecture, Guangxi University of Science and Technology, Liuzhou 545006, China

^b School of Computing, Engineering and the Built Environment, Edinburgh Napier University, 10 Colinton Road, Edinburgh, Scotland EH10 5DT, UK

^c Department of Civil and Environmental Engineering, Faculty of Engineering, Prince of Songkla University, Songkhla 90112, Thailand

^d Construction and Building Materials Research Center, Department of Civil Engineering, King Mongkut's University of Technology North Bangkok, Bangkok 10800, Thailand

^e Department of Civil Engineering, National Yang Ming Chiao Tung University, Hsinchu, Taiwan

^f Department of Construction Technology and Engineering, Technological Higher Education Institute of Hong Kong, 20A Tsing Yi Road, Tsing Yi Island, New Territories, Hong Kong

^g Excellence Center in Infrastructure Technology and Transportation Engineering (ExCITE), Department of Civil Engineering, Chiang Mai University, Chiang Mai 50200, Thailand

^h Department of Civil Engineering, Kwame Nkrumah University of Science and Technology, Kumasi, Ghana

ⁱ Department of Civil and Environmental Engineering, Hong Kong University of Science and Technology, Kowloon, Hong Kong

^j Liuzhou OVM Machinery Co. Ltd., Liuzhou, Guangxi 545005, China

ARTICLE INFO

Keywords:

Prestressed Carbon Fibre Reinforced Polymer
CFRP plate
Structural strengthening
Box girder
Reinforced concrete

ABSTRACT

The paper presents a well-rounded experimental study on the flexural performance of Reinforced Concrete (RC) box girders strengthened with prestressed carbon fibre reinforced polymer (CFRP) plates. The motivation behind the study was twofold: the rising need for structural reinforcement of existing aged and heavily utilised hollow RC box girders, and the absence of prior attempts to integrate prestressed CFRP plate strengthening for those hollow girders. Previous experimental studies are scarce and fewer studies are focused on the combined prestress and thin-wall effects, such as prestress-related stress condensation and shear lag. However, experimental results are important in directing further analytical studies for hollow sections with more complex behaviours than solid sections since there is a need to predict the behaviour of the prestress-strengthened hollow RC structures for routine design. This pivotal experimental study aims to quantify the structural interactions initiated by prestress in hollow sections and evaluate the impact of age while promoting further analytical initiatives. In this study, two types of CFRP plates, ordinary CFRP and steel-wire-CFRP (SW-CFRP), were used on different specimen beams with varying prestressing levels, sizes of the CFRP plates, and pre-damaged states representing aged and over-used members. Their performance indexes, including cracking load, yield load, ultimate load, structural stiffness, ductility, and crack resistance, were tested and summarised in this paper. The CFRP plates of the eight specimen beams were prestressed to different levels (non-prestressed, and 30% and 40% of the CFRP plate's ultimate strength). The test results suggest that the crack load increased by 86% and 134%, when the specimens were enhanced with the combinations of 30% prestress level for the same CFRP cross-section, and 40% prestress level with a thicker CFRP plate, respectively. The flexural capacity also increased by 42% and 72%, and flexural stiffness increased by 3% and 63%, respectively. The experimental results proved that the proposed prestressed CFRP plate technology effectively strengthens the new or aged RC box girders, but the ductility is sacrificed. These first-hand test results provide an excellent target dataset for further development in the analysis and design of prestressed CFRP plate-strengthened RC box girders.

* Corresponding authors.

E-mail addresses: j.zhang@napier.ac.uk (H. Zhang), zouyq@ovm.cn (Y. Zou).

1. Introduction

The application of Reinforced Concrete (RC) box beams, a common structural form being adopted in transportation and other infrastructure systems, can be traced back to a century ago. Many RC box girder structures built several decades ago are still servicing the clients, but traffic loads have become much more demanding. When demolition and re-building may not always be the best option, the alternative approach is always to strengthen and enhance the maintenance of these structures. Among the numerous strengthening methods, carbon fibre rod or plate strengthening has become one of the most popular options due to its outstanding mechanical properties, corrosion resistance, and the benefit of achieving increased strength after being prestressed [1–9]. Prestressed carbon fibre reinforced polymer (CFRP) rods and plates have become one of the engineer's favourite options for strengthening RC structures. However, most previous studies focus on RC beams with a solid cross-section with no previous studies on the hollow sections, such as RC box girders, due to their large member size for spanning long distances and the complexity of test setup (detailed in Section 2).

Wu et al. [10] and Diab et al. [11] conducted experiments to investigate the short and long-term behaviour of the anchorage zones of externally bonded prestressed FRP sheets. The results suggested that through pretension of FRP sheets, significant enhancement can be achieved in the flexural strength, stiffness and crack resistance of strengthened structures. The results also suggested that the creep of adhesive layer leads to loss of the prestress load at high shear stress zones, which also initiates and propagates debonding along the FRP-concrete interface if there is no special anchor. Peng et al. [12] and Tehrani et al. [13] studied the behaviour of RC beams strengthened with externally bonded non-prestressed and prestressed CFRP flexure and prestressed CFRP plates via the externally bonded reinforcement on grooves (EBROG) method. Their experimental results show that the monotonic and fatigue performance of a reinforced concrete beam was significantly enhanced by strengthening with prestressed CFRP plates compared as opposed to strengthening with non-prestressed CFRP plate, and the EBROG technique, in the absence of any end anchorage, was well capable of transferring the prestressing stresses to the beam. Deng et al. [14–17], Zhu et al. [18,19], and Li et al. [20–22] reported on prestressed CFRP plates subjected to sustained loading, continuous wetting conditions, and wetting/drying cycles. Yang et al. [23] and Ehsan [24] studied the flexural performance of RC members strengthened by CFRP plates and employed different bonding and prestressing methods. Through experimental and theoretical analysis, Xue et al. [25] and Emdad and Al-Mahaidi [26] proposed the calculation methods for prestress loss of CFRP plates, the crack resistance capacity of concrete beams strengthened with prestressed CFRP plates. Li et al. [27] and Chang et al. [28] conducted comparative and parametrical studies on RC T-girders and beams strengthened by externally prestressed CFRP plates. Results from destructive tests and refined finite element model analysis indicated the actual ultimate flexural load capacity of the unstrengthened member was 1.58 times the original design load capacity. Zhe-lyazov and Thorhallsson [29] developed a numerical model based on the customized constitutive relationships and failure criteria defined for all the constituencies of the adhesive joint, to simulate the FRP-concrete interface degradation. The proposed model was validated by a benchmark example, a 'angled-peeling test'. Cornetti et al [30] review and compare several analytical models describing the single-lap shear test, which is the most common test to determine the bonding behaviour between a strengthening FRP plates and the concrete substrate. Several conclusions were drawn: 1) the fracture energy is the one that has the strongest influence on the mechanical response of the single-lap shear test; 2) to catch the increment of the debonding load due to increasing bond length, at least two-parameter interface models are needed. Jin et al. [31] studied the size effect of CFRP-wrapped square concrete columns was investigated using both experimental and numerical approaches. The tested square columns exhibit obvious size effect on

Table 1

The mechanical properties of steel reinforcements.

Steel bars	Yield strength	Ultimate strength	Modulus of elasticity	Elongation
Φ8	465 MPa	616 MPa	2×10^5 MPa	26%
Φ10	468 MPa	618 MPa	2×10^5 MPa	34%
Φ20	470 MPa	610 MPa	2×10^5 MPa	28%

Table 2

Mechanical properties of concrete (MPa).

Concrete type	Modulus of elasticity	Compressive strength	Tensile strength
C40	3.35×10^4	46.8	2.85

nominal compressive strength and the displacement ductility coefficient decreases significantly as the structural size increases. Heydarinouri et al. [32] developed a new retrofitting system to reduce the out-of-plane deformation of the connections using prestressed CFRP rods. The proposed system was found to be capable of reducing the stresses at the angle connections by more than 40%. A few studies [33–35] focused on using CFRP rods (prestressed or non-prestressed) to replace steel reinforcement or prestressing tendons for reinforced box beams. Although CFRP rods encased in the concrete as normal reinforcements or tendons is not classed as a strengthening method, it is a creative application of CFRP rods in box beams.

Prestressed CFRP plate has great potential in RC structure strengthening and has attracted much research attention in recent years. However, most previous studies focused on structural members with solid cross-sections, such as rectangular RC beams or RC T beams. It can be seen that 1) no studies have focused on the prestressed CFRP plate strengthening of structural members with a hollow section, such as RC box girders; and 2) there are no experimental studies that can demonstrate the effectiveness and validate the strengthening method for this type of girder with a more complex cross-section. For hollow RC box structures, the demand for structural maintenance and strengthening in the case of aging and deterioration are higher than with other types of structures. Prestressed CFRP plate strengthening does provide a competitive approach for this purpose. Addressing these gaps will also pave the way for developing an analytical method for analysing and designing these structural members to guide engineers to adopt this technology.

An experimental study was conducted to develop prestressed CFRP strengthening methods for RC box girders. Two types of CFRP plates were used: ordinary CFRP and steel-wire-CFRP (SW-CFRP). A total of eight RC box girders were manufactured and tested. Full detailed are listed in Table 1 of the companion paper [9]. Two of the eight samples were pre-loaded to partially damaged/cracked status, gauged by the strain of tensile reinforcement; 60% and 80% of the yield strain for SSL1A-3P and SSL1B-4P, respectively. The level of pre-load is controlled by the strain reading from the strain gauges attached to the tensile reinforcement. The specimen with the tensile reinforcement "pre-strained" to 60% yield strain would be approaching the elastic-plastic transition. Meanwhile, the specimen would be approaching the ultimate state in practical design when its tensile reinforcement reaches 80% yield strain. The structural performances of these samples were evaluated using the four-point bending test. The specimen beams' performance indexes were tested and summarised in this paper, including cracking load, yield load, ultimate load, structural stiffness, ductility, and crack resistance (Table 2 and Table 3).

Table 3
CFRP specifications and material properties.

Type	Specification(mm × mm)	Tensile strength	Ultimate breaking force	Modulus of elasticity	Elongation %
OVM.CFP50-2	50 × 2	≥2400 MPa	≥240kN	≥160GPa	≥1.6
OVM.CFP50-3	50 × 3	≥2400 MPa	≥360kN	≥160GPa	≥1.6
GJ.CFP50-3	50 × 3	≥1466 MPa	≥270kN	≥160GPa	≥4.0

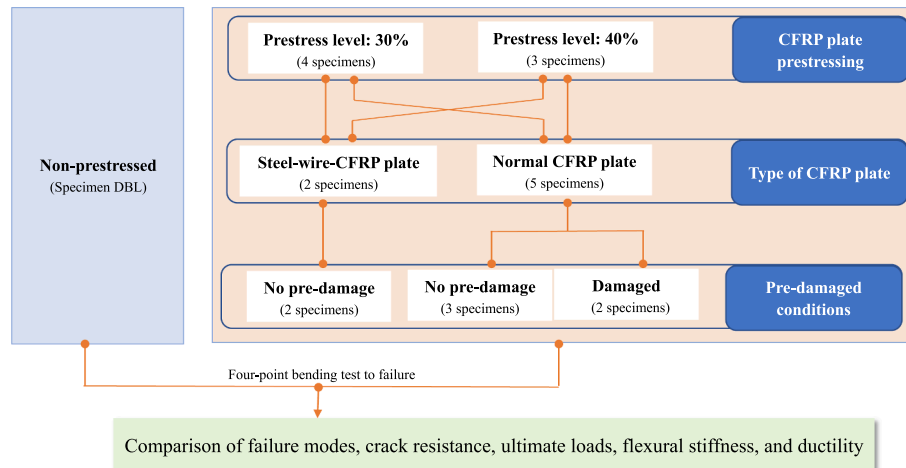


Fig. 1. Flowchart of the proposed experimental study.



Fig. 2. Strain gauges attached on the bottom tensile reinforcements.

2. Experiment design and test procedure

2.1. Test design and sample preparation

A total of eight specimens of RC box girder were designed and fabricated for the experiment. The flowchart of the proposed experimental study is shown in Fig. 1. The specification of the specimen beams is shown in Fig. 1 of the companion paper [9]. In this study, four-point bending test method is employed to investigate the flexural behaviours of the box girders strengthened by CFRP plates. The beams tested in the four-point bending test possess a pure bending segment in which the flexural capacity, deflection, and crack propagation were investigated and measured. Although some of the design details below have been presented in the companion paper [9], for sake of completeness of this paper, a complete design specification are detailed below. The total length of each specimen is 3600 mm, and the loading span is 3400 mm. The concrete grade is C40, and the tensile and compression reinforcements are 4Φ20 and 5Φ10 HRB400 steel rebar, respectively. The longitudinal reinforcement of web components on both sides of the girders is 2Φ8 HRB400 steel reinforcement. Shear stirrups of Φ10@200 c/c are provided within the middle portion (1 m long between two loading points) to prevent the members from suffering shear failure during the four-point bending tests. The remaining portions (each 1.2 m long between a loading point and the nearest support) are provided with

stirrups of Φ10@100 c/c. The steel grade of the stirrups is also HRB400. The reinforcement details and test setup are specified in Fig. 1 of the companion paper [9]. Strain gauges were attached to the bottom tensile reinforcements at mid-span and loading-point locations (Fig. 2) before being assembled to form the completed reinforcement cages (Fig. 3). The reinforcement cages were then placed into the formwork for concrete casting (Fig. 4). The size and dimensions were chosen with consideration for the maximum capacity of both testing and manufacturing facilities.

The CFRP plates and tailor-made clamps were provided by Liuzhou OVM Machinery Co, Ltd (OVM). Three types of CFRP plates were used, namely models OVM.CFP50-2, OVM.CFP50-3 and GJ.CFP50-3, the most commonly used products manufactured by Liuzhou OVM Machinery CO. Ltd. The adhesive used in this study was Lica-131A/B carbon fibre composite impregnated adhesive (fibre composite structural adhesive) and was manufactured by Nanjing Hitech Composite Material Co., LTD. The cross-section areas, tensile control stress, and the materials that CFRP plates are made of were among the key considerations of the design in this experimental study. The parameters of the test design for this study are shown in Table 1 of companion paper [9], and the schematic diagram of the CFRP plate prestressing device is shown in Fig. 5. The material properties of the steel rebar, concrete, and CFRP are shown in Table 1 to Table 4. Fig. 6 shows the CFRP plate before loading and after failure in a loading test. The CFRP plates all exhibited a unique

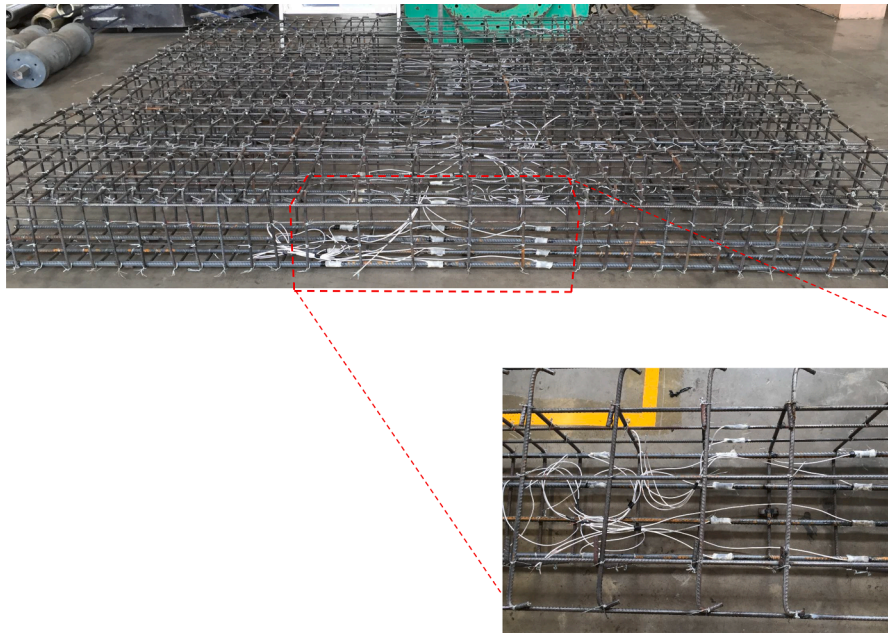


Fig. 3. Completed reinforcement cages with strain gauges attached.



Fig. 4. Formwork for box girder concrete casting.

gradual filamentary failure presented with an explosive effect, as shown in Fig. 6. A similar phenomenon was observed at the final stage of the rupture tests for the CFRP-strengthened beams.

Three types of specimens were designed and fabricated to simulate the three common practical scenarios determined from existing engineering applications:

- (1) Non-strengthened control beams (series DBL) to simulate the normal RC box girder beams.
- (2) Box beams strengthened with different types of CFRP plates and under varying levels of prestress (series JGLx-xx) to simulate and validate the proposed prestressed CFRP plate strengthening methods on RC box girder beams.
- (3) Pre-loaded (partially damaged) box beams strengthened with CFRP plate with different levels of prestress (series SSLxx-xx) to simulate the application of the proposed prestressed CFRP plate

strengthening methods on the aged, over-used RC box girder beams.

The DBL (control) beam was utilised as a benchmark for evaluating the effectiveness of the other beams' strengthening methods. The JGL beams are RC box girders with prestressed normal and SW-CFRP plates. SSL beams were included in the test group to investigate the impact of utilising prestressed normal CFRP plates on partially damaged (cracked) beams. The CFRP plates were prestressed and installed following the step-by-step procedures specified by the manufacturer. The bending test followed the standard four-point flexural test with two evenly spaced point loads applied from the reaction ends.

The prestressing and installation of CFRP plates were carried out with the facilities in Liuzhou OVM Machinery Co., LTD. The detailed procedure was presented in Section 2.1 of the companion paper [9].

2.2. Test procedure and loading scheme

Specimens with less than 50-ton ultimate load capacity were tested on an MTS 50T hydraulic Servo System. The specimens were loaded through a spreader beam which evenly distributed two point-loads 1 m apart onto the middle section of the specimen beams. After being strengthened by a CFRP plate, some specimens would have an ultimate load capacity near or exceeding the 50-ton and thus be tested on an MTS 100T hydraulic Servo System instead. The tests using MTS hydraulic Servo Systems are shown in Fig. 7.

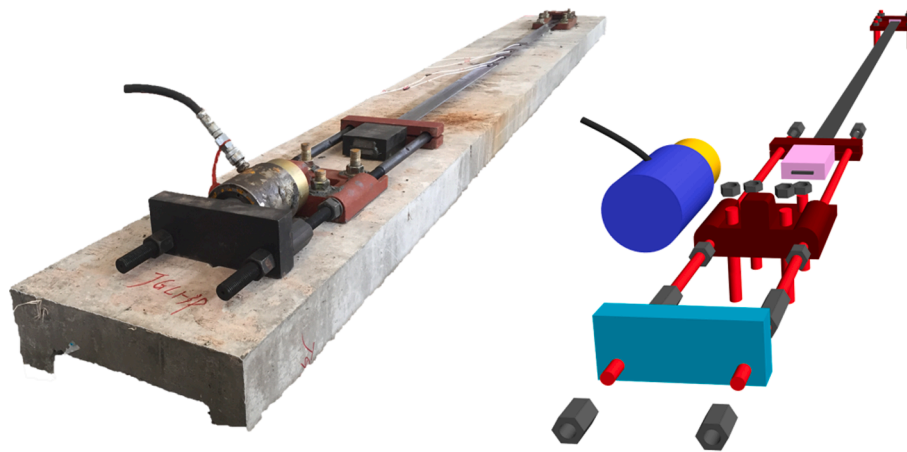
The test followed a hierarchical loading scheme. The detailed loading procedure was presented in Section 2.2 of the companion paper [9].

3. Test results and analysis

The test results and failure characteristics are shown in Table 5. P_{cr} is the load value when the first crack was observed, P_y is the load value when the longitudinal tensile reinforcement yielded, and P_{max} represents the ultimate load. α_{cr} , α_y and α_{max} respectively represent the ratio of the above cracking, yielding and ultimate load of the strengthened beam to the corresponding value of the control beam (DBL). Δ_y and Δ_u are the mid-span deflection of the corresponding reinforcement under yield and ultimate load, respectively. $P_{L/400}$, $P_{L/300}$, $P_{L/200}$ are the loads



(a) Prestress device and setup



(b) Details and exploded view of the prestress device and setup

Fig. 5. Schematic diagram of the prestressed CFRP plate device.

Table 4
Structural adhesive product specification.

Structural adhesive	Compressive strength (MPa)	Tensile bonding strength (MPa)	Steel to steel shear strength (MPa)
Lica-131A/B	92	4.2	27

when the mid-span deflection reached $L/400$, $L/300$, and $L/200$, where L is the span of the specimen beam. $\alpha_{L/400}$, $\alpha_{L/300}$, $\alpha_{L/200}$ are the ratios of these loads to the corresponding value of the control beam (DBL). Mid-span deflection at $L/400$, $L/300$, and $L/200$ are also the empirical figures of flexural deformation at elastic, elastic-plastic, and maximum allowable deflection at the serviceability limit state.

3.1. Load-deflection curves and failure characteristics

The failure modes of each beam were shown in Fig. 3 of the companion paper [9] with the following observations summarised in this paper:

- (1) The failure mode of control beam DBL is typical flexural/bending failure, i.e., the concrete in the compression zone is crushed after the tensile reinforcements yield. The beam began to yield when the tensile reinforcement strain reached $2365 \mu\epsilon$, and then the deformation continued to increase. When the beam was loaded to 318 kN, the compressive concrete was crushed, and the specimen failed.
- (2) The flexural capacity of beams JGL1-3P and JGL1-4P are significantly improved compared with that of non-strengthened beams, and the crack spacing and width were also less than that of the control beam. When the strain of the tensile reinforcement reached $2350 \mu\epsilon$, it began to yield. Meanwhile, cracks appeared in the concrete, and a continuous sound was emitted from the CFRP plate. The CFRP plate was broken when the ultimate load was reached.
- (3) The flexural capacity of beam JGL2-4P noticeably improved compared with the beams JGL1-3P and JGL1-4P, as well as its resistance to cracking. When the strain of the tensile reinforcement reached $2358 \mu\epsilon$, the concrete began to yield and sizzle. The specimen failed when loaded to 548 kN, with the concrete in the compression zone peeled and crushed.



Fig. 6. Uniaxial loading tests for CFRP plates.



Fig. 7. Four-point bending test setup.

- (4) The beams JGL3-3P and JGL3-4P are strengthened by a CFRP plate blended with high-strength steel wire (SW-CFRP plate). The CFRP plates were prestressed before being attached to the box beams. Their flexural capacity was slightly lower than beam JGL2-4P, and the crack resistance was similarly low. When the strain reached $2353 \mu\epsilon$, the tensile reinforcement began to yield, and the concrete cracked. The CFRP plate emitted a sizzling sound as the load continuously increased until the high-strength steel wire in the SW-CFRP plate snapped, resulting in continuous miniature shock vibrations. The CFRP plate fractured in filamentary failure when the ultimate load was reached.
- (5) The beams SSL1A-3P and SSL1B-4P were loaded until the strain of the tensile reinforcement reached 60% and 80% of its yield strain, respectively, to create a pre-damage status and then they were unloaded completely before being strengthened with prestressed CFRP plates. Compared with the non-strengthened control beam, the crack propagation rates in SSL1A-3P and SSL1B-4P were reduced. Under the same load, crack spacing and width were significantly reduced. When the ultimate load was reached,

the CFRP plates, again, fractured in filamentary failure. This result proves that the prestressed CFRP plate strengthening method is effective for aged and over-used box girder beams. It can improve the ultimate flexural capacity, enhance the crack resistance and, ultimately, extend the duration of service.

The load–deflection curves of the midspan section of the eight test beams were presented in Fig. 4 of the companion paper [9] as a reference for analytical study. The observations of the experimental result are summarised below.

The load–deflection curve of the beams can be divided into three stages: elastic, elastic–plastic, and failure.

- (1) The elastic stage ranges from the beginning of loading to the stage when the first crack in the concrete is observed. In this stage, the concrete has not cracked yet. Therefore, the steel bars, concrete, and CFRP plate act jointly to withstand the tensile stress in the tensile zone, and all materials are assumed to be in the elastic stage.
- (2) The elastic–plastic stage starts from the first crack in the concrete to the yielding of the reinforcement in the tensile zone. During this stage, the cracks redistribute the aggregated tensile force in the tension zone from the concrete to the steel bar and CFRP plate. The strain increases faster than in the first stage until the steel bars in the tension zone yield. The overall flexural stiffness of the test beam starts to decrease. However, the recorded load–strain curve for tensile reinforcement and CFRP plate, as shown in Fig. 10 and discussed later, shows no sign of weakening.
- (3) The failure stage starts right after the tensile reinforcement yield and lasts until the final failure of the member. After the tensile reinforcements yield, the overall flexural stiffness of the test beam continues to decrease. In this stage, the slope of the load–strain curve of the CFRP plates and tensile reinforcement suggests an apparent weakening compared to the second stage. The CFRP plate essentially sustains the longitudinal tensile force. As the load continues to increase, the strain of the CFRP plate continues to increase until it reaches the ultimate capacity.

Table 5
Measurements and test results.

Specimen No.	p_{cr} (kN)	α_{cr}	p_y (kN)	α_y	p_{max} (kN)	α_{max}	Failure mode		
DBL	60.02	1.00	251	1.00	318	1.00	Tensile steel yielded; compression zone concrete crushed		
JGL1-3P	111.35	1.86	362	1.44	453	1.42	Tensile steel yielded; CFRP plate broke		
JGL1-4P	123.45	2.06	372	1.48	469	1.47	Tensile steel yielded; CFRP plate broke		
JGL2-4P	140.65	2.34	432	1.72	548	1.72	Tensile steel yielded; compression zone concrete crushed		
JGL3-3P	127.22	2.12	395	1.57	505	1.59	Tensile steel yielded; CFRP plate broke		
JGL3-4P	131.22	2.19	404	1.61	515	1.62	Tensile steel yielded; CFRP plate broke		
SSL1A-3P	/	/	340	1.35	450	1.42	Tensile steel yielded; CFRP plate broke		
SSL1B-4P	/	/	351	1.40	449	1.41	Tensile steel yielded; CFRP plate broke		

Specimen No.	$P_{L/200}$ (kN)	$\alpha_{L/200}$	$P_{L/300}$ (kN)	$\alpha_{L/300}$	$P_{L/400}$ (kN)	$\alpha_{L/400}$	Δ_y (mm)	Δ_u (mm)	Δ_u/Δ_y
DBL	240	1.00	162.6	1.00	124.5	1.00	17.92 mm	111.00	6.19
JGL1-3P	251.4	1.05	167	1.03	128.5	1.03	24.78 mm	60.56	2.44
JGL1-4P	255.9	1.07	177.9	1.09	131	1.05	23.47	45.00	1.92
JGL2-4P	373.3	1.56	259.2	1.59	203.3	1.63	21.32	41.65	1.95
JGL3-3P	287.5	1.20	201.7	1.24	158	1.27	28.10	57.98	2.06
JGL3-4P	295.5	1.23	208.6	1.28	166	1.33	27.56	55.01	2.00
SSL1A-3P	264.8	1.10	182.9	1.12	128.7	1.03	23.53	58.56	2.49
SSL1B-4P	307.2	1.28	209.3	1.29	152.9	1.23	20.43	42.23	2.07

3.2. Loading stages and measurements

3.2.1. Cracking load

In a previous study, Shang et al. [36] suggested that the non-prestressed CFRP strengthening method does not increase the cracking load. However, with the prestressed CFRP plate, the cracking load was increased significantly in this study. Compared to the cracking load of the DBL control beam, the cracking loads of JGL1-3P, JGL1-4P, and JGL2-4P (strengthened by ordinary prestressed CFRP plates) are 111.35 kN, 123.45 kN, and 140.65 kN respectively, i.e., 86%, 105% and 134% higher than DBL (60.02kN). The cracking loads of JGL3-3P and JGL3-4P (strengthened by prestressed SW-CFRP) are 127.22 kN and 131.22 kN, respectively, 112% and 119% higher than the control beam. It is evidenced that the prestressing effect has applied an extra restraint on the tension zone of the concrete through the CFRP plates (ordinary or steel wire enhanced), which resulted in a significant increase in cracking load. This prestress-induced bottom tension in the CFRP plate also created a “pre-camber” equivalent scenario by bowing the specimen beam upwards and applying the pre-compression stresses in the concrete tension zone to counteract the cracking load applied. This observation has proven the advantage of using the prestressed CFRP strengthening methods. It can reduce the cracks and crack propagation in the box girder beams and thus increase or extend the duration of service.

3.2.2. Yield load and maximum flexural capacity

The yield load and the ultimate flexural capacity of each test beam are given in Table 5. The yield load of the control beam is 251 kN, while JGL1-3P, JGL1-4P, and JGL2-4P are 362 kN, 372 kN, and 432 kN, increased by 44%, 48%, and 72%, respectively, compared to DBL. The yield loads of JGL3-3P and JGL3-4P are 395 kN and 404 kN, respectively, 57% and 61% higher than DBL. Under the same level of prestress, the yield load of the test beam increases with higher amounts of reinforcement. With the same level of reinforcement, the yield load of the test beam increases slightly with a greater level of prestressing, i.e., the “prestressing effect” on member yield load is lower than that caused by the amount of reinforcement. The ultimate flexural capacity of DBL is 318 kN, while the maximum flexural capacities of JGL1-3P, JGL1-4P, and JGL2-4P are 453 kN, 469 kN, and 548 kN, respectively; an increase of 42%, 47% and 72% against the DBL benchmark. The ultimate flexural capacities of JGL3-3P and JGL3-4P are 505 kN and 515 kN, respectively, i.e., 59% and 62% higher than the control beam. In conclusion, while both methods can enhance the ultimate flexural capacity of the specimen beam, increasing the reinforcement area proves to be more effective than increasing the prestressing level.

Comparing JGL2-4P and JGL3-4P, the test beams' yield load and

ultimate flexural capacity strengthened with ordinary CFRP plates is higher than when strengthened with steel-based SW-CFRP plates. The main reason is that the high-strength steel wires weaved in the CFRP board snapped earlier than the carbon fibre, resulting in non-uniform stress distribution and early fracture.

The yield loads of SSL1A-3P and SSL1B-4P were 340 kN and 351 kN, respectively, increasing 26% and 29% compared with DBL. However, when comparing members SSL1A-3P, JGL1-3P, SSL1B-4P, and JGL1-4P, the strain of the reinforcement in the tensile zone increases with the degree of pre-damage before strengthening, thus leading to an early yielding of the tensile reinforcement and a reduced yield load. The ultimate flexural capacities of SSL1A-3P and SSL1B-4P are 450 kN and 449 kN, respectively, 42% higher than that of DBL. The higher the pre-damage level applied (specimen SSL1B-4P in this case), the earlier the CFRP plate failed. The ultimate flexural capacity is also smaller than specimen beams without pre-damage (JGL1-3P and JGL1-4P).

3.3. Section stiffness

As shown in Table 5, the $P_{L/400}$ of DBL is 124.5 kN, while JGL1-3P, JGL1-4P, and JGL2-4P are 128.5 kN, 131 kN, and 203.3 kN, respectively, which are 3.2%, 5.2%, 63.3% higher than DBL. The $P_{L/300}$ of DBL is 162.6 kN, while JGL1-3P, JGL1-4P, and JGL2-4P are 167 kN, 177.9 kN, and 259.2 kN, respectively, i.e., 2.7%, 9.4%, 59.4% higher than DBL. The initial stiffness of JGL1-3P and JGL1-4P is slightly higher than DBL, while the initial stiffness of JGL2-4P is significantly higher. This result is due to the larger CFRP plate cross-section and higher prestress level. The $P_{L/400}$ of JGL3-3P and JGL3-4P are 158 kN and 166 kN, respectively, which are 26.9% and 33.3% higher than DBL, and the $P_{L/300}$ of JGL3-3P and JGL3-4P are 201.7 kN and 208.6 kN, respectively, which are 24% and 28.3% higher than DBL. Thus it is clear that their initial stiffness was significantly increased. A similar situation is observed for $P_{L/200}$, as shown in Table 5.

Therefore, the test results suggest that increasing the CFRP plate's cross-section improves the specimen beam's stiffness. Increasing the level of prestressing had a similar effect but was less obvious. The main reasons why increasing the CFRP cross-section area or prestressing the CFRP plate can improve the stiffness are as follows:

- (1) The prestressing effect formed a local arch with the CFRP plate and adjacent concrete. The arch effect reduced the crack propagation and increased the section's moment of inertia, thus increasing the overall equivalent flexural stiffness and decreased deflection.

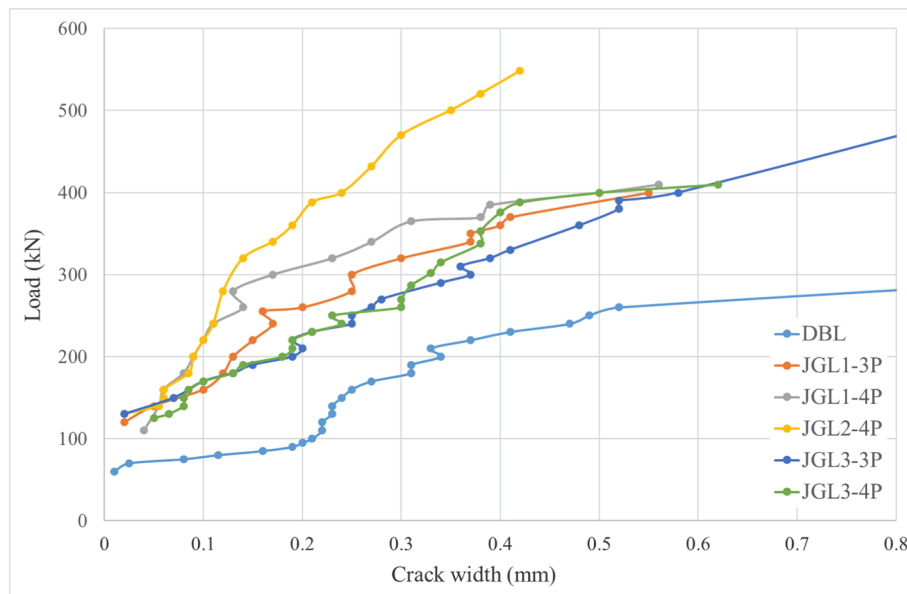


Fig. 8. Loads vs crack widths plot for beams with different configurations.

(2) The additional CFRP plate attached is equivalent to increasing the reinforcement area in the tensile zone, which improves the stiffness of the beam. It is noted that the ordinary CFRP plate enhanced flexural stiffness more than the SW-CFRP plate did because the elastic modulus of the steel wires is smaller than the carbon fibre. Hence, the SW-CFRP plate provided less equivalent reinforcement area than a CFRP plate of the same size.

3.4. Failure modes

Fig. 8 summarises the load-crack curves of each test beam (the crack width was measured on the main crack width). The crack propagation can generally be divided into three stages: (1) The first stage is from the first crack to forming a stable crack pattern with almost no further new cracks appearing. At this stage, the rate of increase of the main crack width is relatively steady and gentle. (2) The second stage is mainly dominated by the further development of the existing cracks. The crack propagation rate is faster than the first stage but not significantly. (3) At the final stage, the crack width increases rapidly until the final rupture failure of the specimen beam. More detailed observation is summarised below.

When the load applied was increased to 100 kN, the average crack width of DBL was 0.21 mm, while no crack was observed for JGL1-3P, JGL1-4P, JGL2-4P, JGL3-3P, and JGL3-4P at this level of loading. When the load increased to 200 kN, the crack widths of DBL, JGL1-3P, JGL1-4P, JGL2-4P, JGL3-3P, and JGL3-4P were 0.33 mm, 0.13 mm, 0.09 mm, 0.09 mm, 0.18 mm, and 0.13 mm, respectively. When the load reached 300 kN, DBL had already failed, and the crack widths of JGL1-3P, JGL1-4P, JGL2-4P, JGL3-3P, and JGL3-4P were 0.25 mm, 0.17 mm, 0.13 mm, 0.33 mm, and 0.25 mm, respectively. Prestressed CFRP strengthening methods can effectively improve the crack resistance of the RC box girder beam. Moreover, increasing the prestressing level will result in higher crack resistance after strengthening, and the ordinary CFRP performs better in crack prevention than the SW-CFRP.

The crack patterns were recorded and are illustrated in Fig. 9, and the distributions of the cracks reveal that:

(1) Comparing JGL1-3P, JGL1-4P, JGL3-3P, and JGL3-4P with different levels of prestressing, the main crack widths decrease significantly with increasing levels of prestressing. The crack

propagation rate also becomes slower and steadier with a higher prestressing level.

- (2) While comparing JGL1-4P and JGL2-4P, JGL2-4P (with a thicker CFRP plate attached) achieved a better crack resistance evidenced by a slower crack propagation and less dense crack pattern.
- (3) Comparing the crack patterns of JGL2-4P and JGL3-4P again proves the CFRP plate performs better than the SW-CFRP plate in enhancing the crack resistance of the box girder beams.
- (4) By comparing SSL1A-3P, SSL1B-4P, and DBL, their crack patterns proved the outstanding performance of the prestressed CFRP plate strengthening methods, even for RC box girder beams with pre-damaged conditions.

This experimental result also confirmed the potential of this method for structural strengthening and retrofitting for aged and over-used RC box girder structures.

3.5. Load-strain curves

The load-strain curves of the main tensile reinforcement, the concrete surface at the top middle of the specimen beam, and the CFRP plates of each test beam are shown in Fig. 10. A noticeable difference among all the curves is that the strain of the concrete compression zone, represented by the measurement at the top-middle surface of the DBL beam, increases the most rapidly, followed by JGL3-3P and JGL3-4P (strengthened with SW-CFRP plate); JGL1-3P, JGL1-4P, and JGL2-4P (strengthened by ordinary CFRP plate) are among the slowest. The prestressed CFRP plates can reduce the strain increase rate through the coupled composite and prestressing effect between the CFRP plate and concrete box girder. Compared to the SW-CFRP plates, the ordinary CFRP plates are more effective in slowing down the crack propagation and preventing the cracks from pushing up to reduce the concrete's compression zone, resulting in low compressive stress.

Fig. 10 also reveals that for beams JGL1-3P, JGL1-4P, JGL2-4P, JGL3-3P, and JGL3-4P, the strains of the CFRP plates were very small and made almost no contribution towards the flexural capacity before the cracking load. When the tensile reinforcement reached its yielding point, the resultant tensile force in the tensile zone was mainly borne by the steel reinforcement and the CFRP plate. The strains of the CFRP plates for the beams listed above were around $3293\mu\epsilon$, $3231\mu\epsilon$, $2869\mu\epsilon$,

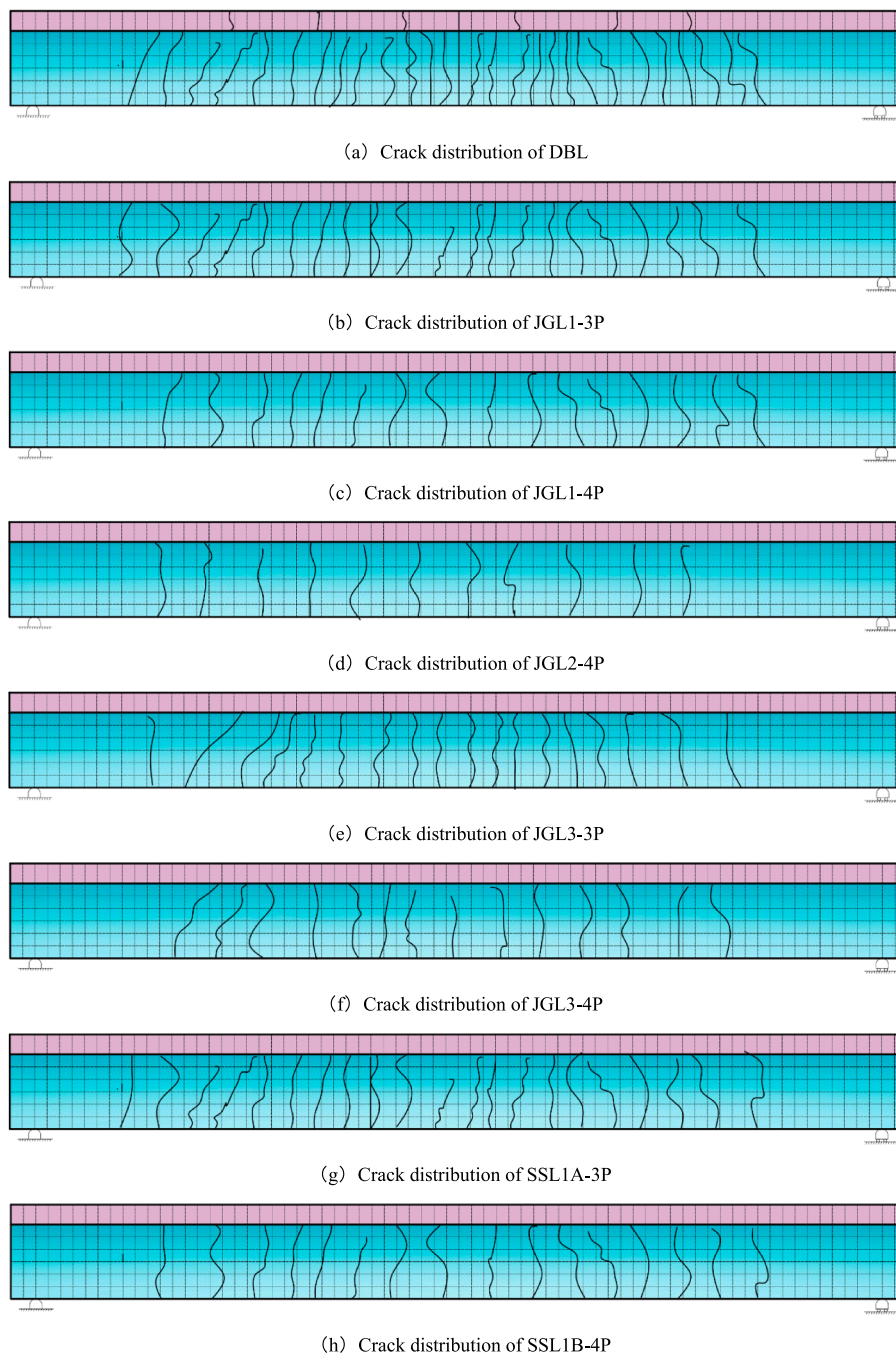
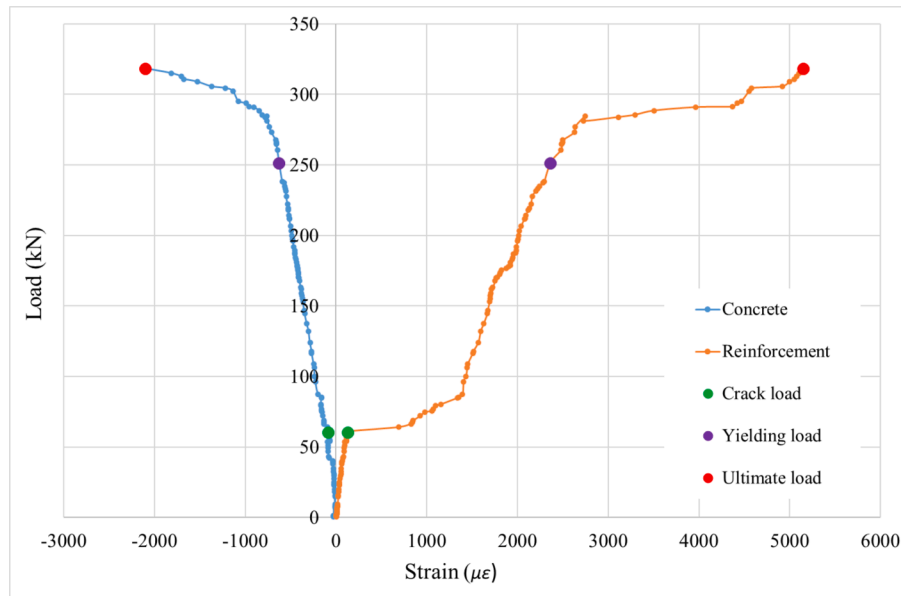


Fig. 9. Crack distribution of the test beams.

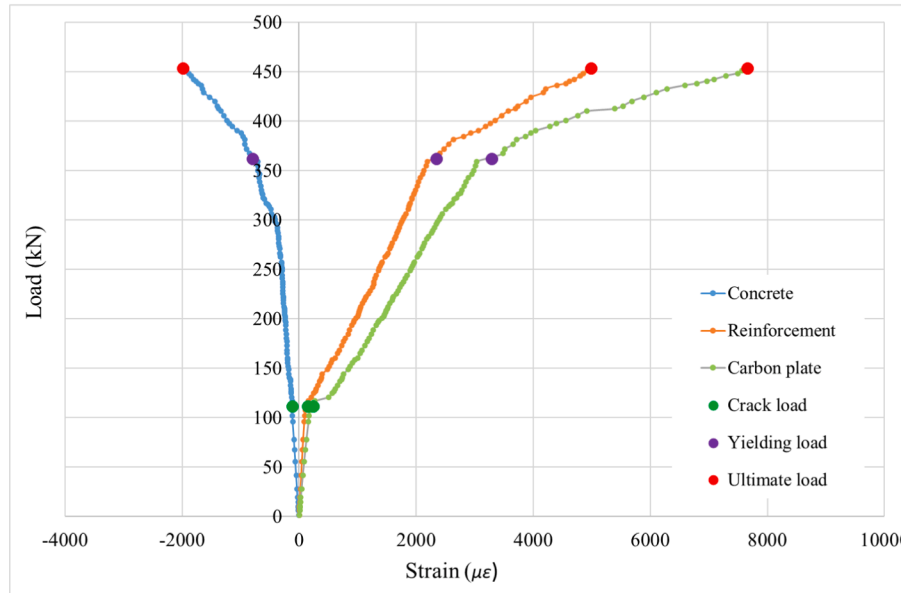
2527 $\mu\epsilon$, and 3321 $\mu\epsilon$, respectively, consuming only 21.9%, 21.5%, 19.1%, 27.6%, and 36.2% of the ultimate strain. After the tensile reinforcement yielded, the CFRP plate played an even more important role by taking on a greater share of the force in the tensile zone. When the tensile reinforcement reached the ultimate state, the tensile strains of the CFRP plates were 7670 $\mu\epsilon$, 8879 $\mu\epsilon$, 5689 $\mu\epsilon$, 8333 $\mu\epsilon$, and 7276 $\mu\epsilon$, respectively, and utilised around 81.1%, 99.2%, 77.9%, 98.4%, and 97.2% of the CFRP plates' ultimate strains, respectively, after adding on the prestressed strain. The final failure mode of JGL2-4P is concrete crushing in the compression zone, while the final failure modes of JGL1-3P, JGL1-4P, JGL3-3P, and JGL3-4P are all tensile failure of CFRP plates.

SSL1A-3P and SSL1B-4P were loaded until the strain of the tensile reinforcement reached 60% and 80% of the yield strain, respectively, and then were fully unloaded before being strengthened with

prestressed CFRP plates. As shown in Fig. 10 (g) and (h), the tensile reinforcement yielded at 340 kN and 351 kN load, respectively, while the strain of the CFRP plates was 3215 $\mu\epsilon$ and 3190 $\mu\epsilon$, utilising 21.4% and 21.3% of the ultimate strain. Comparing pre-damaged specimens (i. e., SSL1A-3P and SSL1B-4P) with the corresponding non-damaged specimens (i. e., JGL1-3P and JGL1-4P), there is only a very small difference in strain at this stage but a significant drop in yield loads. This result indicates that the pre-formed damage affects the stress level of the tensile reinforcement in the tensile zone but will not affect the stress level in the CFRP plates. Comparing the yield levels of non-damaged specimens with their corresponding pre-damaged ones, the tensile reinforcement of the pre-damaged beams yielded earlier. At the ultimate limit state, the compressive strain of concrete reaches $-1862\mu\epsilon$ and $-2175\mu\epsilon$ and the tensile strain of the CFRP plate reaches 8893 $\mu\epsilon$ and



(a) DBL



(b) JGL1-3P

Fig. 10. Load-strain relationship measurements of steel bar, concrete and CFRP plate of specimen beams.

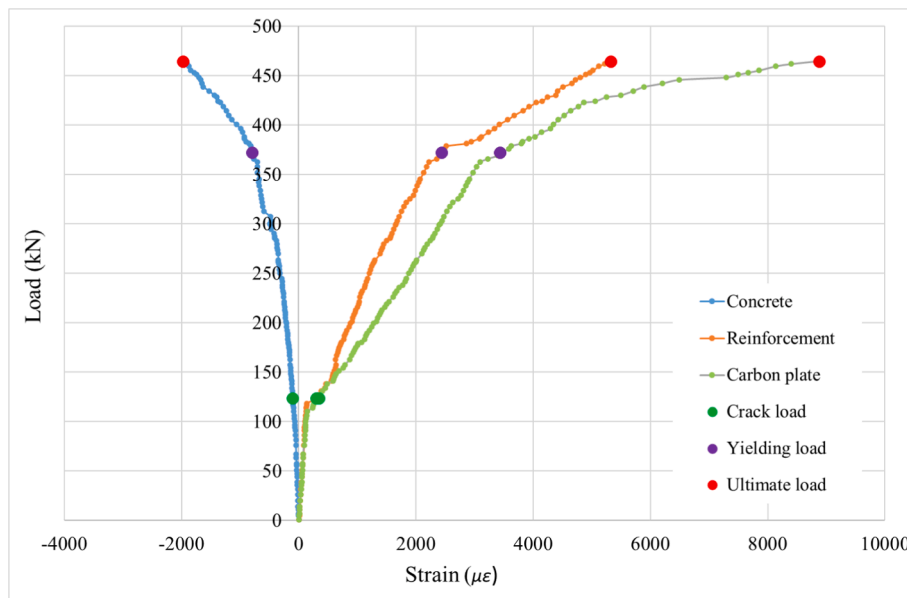
7199 $\mu\epsilon$, with 89.3% and 88% of ultimate strain utilised after adding on the prestressed strain.

3.6. Ductility

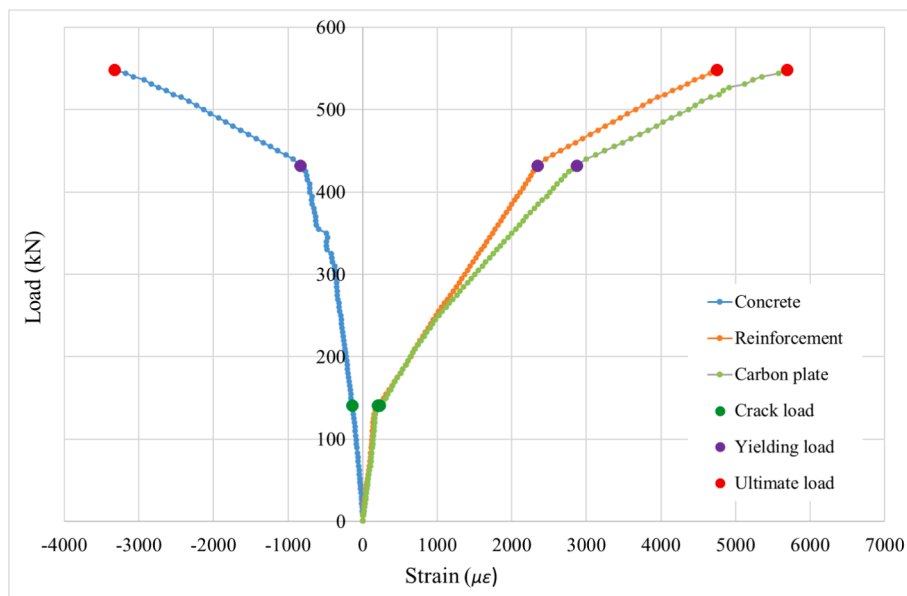
The stress-strain relationship of CFRP materials is a typical full-range linear elastic relationship with a brittle failure at the end, and it has no plastic deformation. Therefore, attaching a CFRP plate would adversely affect the ductility of the strengthened concrete box girder beams. The ductility index is often used to describe the ductility of structures, which is the ratio of the ultimate deflection and the yield deflection of the component or structure. The higher the ductility index, the better the structure's ductility. The yield deflection, Δ_y , is defined as the corresponding deflection of tensile steel yield in the box girder, while the limit deflection, Δ_u , is defined as the deflection corresponding to the ultimate load of the final failure. In this study, the limit deflection

is marked by either concrete crushing in the compression zone or the prestressed CFRP plate snapping. As shown in Table 5, the ductility index of the control beam, DBL, is 6.19. The ductility indexes of JGL1-3P, JGL1-4P, and JGL2-4P are 2.44, 1.92, and 1.95, respectively, while the ductility indexes of JGL3-3P and JGL3-4P are 2.06 and 2.00, respectively. The following conclusions can be drawn from the test results:

- (1) Compared with the non-strengthened control beam, the ductility of prestressed CFRP-reinforced beams is greatly reduced.
- (2) With the same prestressing level, the ductility decreases as the total cross-sectional area of the CFRP plates increases. While with the same size of CFRP plates, the ductility decreases as the level of prestressing increases.



(c) JGL1-4P



(d) JGL2-4P

Fig. 10. (continued).

- (3) Comparing the results of beams JGL2-4P and JGL3-4P, the SW-CFRP plate offered better ductility to the strengthened box girders than the ordinary CFRP plate.

4. Conclusions

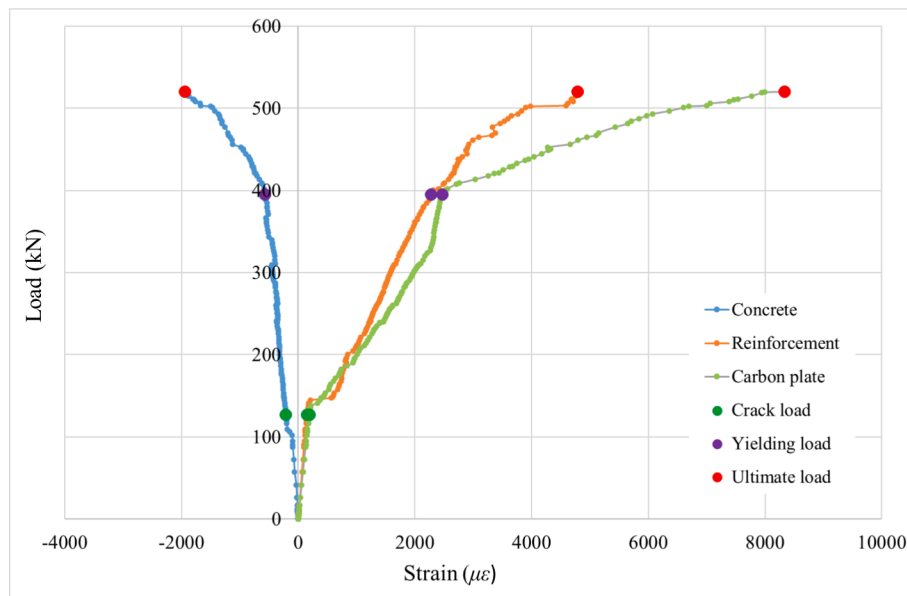
This experimental study demonstrated the advantages and shortcomings of using the prestressed CFRP plate technology to strengthen new or aged RC box girders. The following conclusions were drawn within the limited scope of this study.

The prestressed CFRP plate strengthening methods can effectively enhance the flexural capacity, crack resistance, and structural stiffness of new or aged (simulated by the pre-damaged specimen beams) RC box girder beams, with the cost of sacrificing the ductility of the girder. The ultimate flexural capacity was significantly increased when strengthening the pre-damaged specimen beams but less so than the strengthened normal specimen beams.

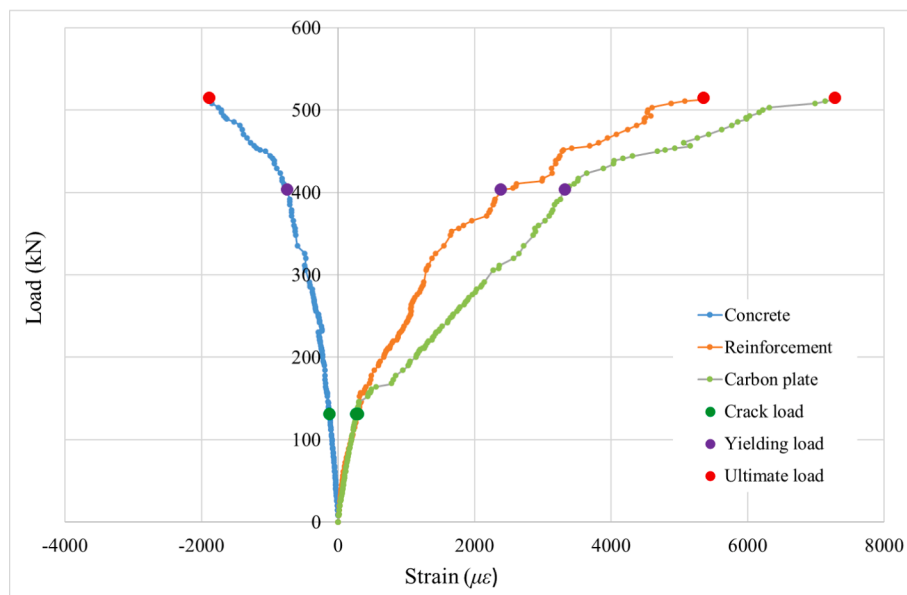
The CFRP plate's cross-sectional area and the prestressing level are the key elements influencing several key performance indexes, such as cracking load, yield load, ultimate load, structural stiffness, and crack resistance. Increasing the cross-sectional area of the CFRP plate and the prestressing level can improve the above performance, but increasing the prestressing level is more cost-effective.

The performance of the SW-CFRP plate is slightly lower than the ordinary CFRP plate: around 10% smaller in yield load and ultimate load. However, the SW-CFRP plate costs much less than the ordinary CFRP plate. Thus, it is a good alternative material for box girder strengthening.

The test results reveal that around 80%-100% of the CFRP capacity and a maximum of 90% of the SW-CFRP capacity were utilised in the rupture tests. Considering that the CFRP and SW-CFRP plates both failed or were close to failure at the point of rupture, the optimum composite combination selected, i.e., 30% to 40% of the CFRP and SW-CFRP plates' ultimate strength, for the prestress level in this study are adequate.



(e) JGL3-3P



(f) JGL3-4P

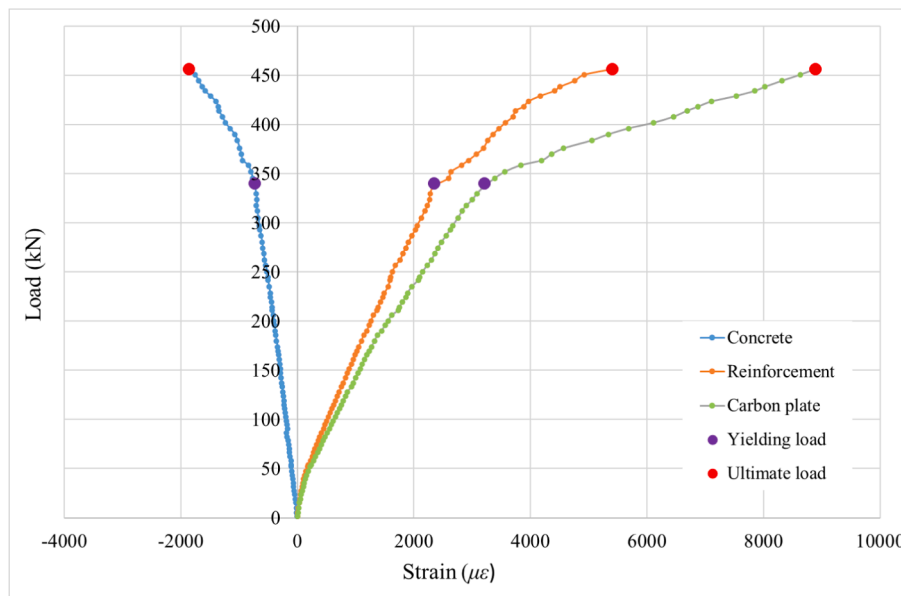
Fig. 10. (continued).

The test results indicate that the prestressed specimens, JGL1-3P and JGL2-4P, which have 30% and 40% equivalent CFRP plate ultimate strength prestress levels, and 50x2 mm and 50x3 mm CFRP cross-section, respectively, show an 86% and 134% increase in crack load when compared to the non-prestressed specimen (DBL). The flexural capacity also increased by 42% and 72%, and flexural stiffness increased by 3% and 63%, respectively.

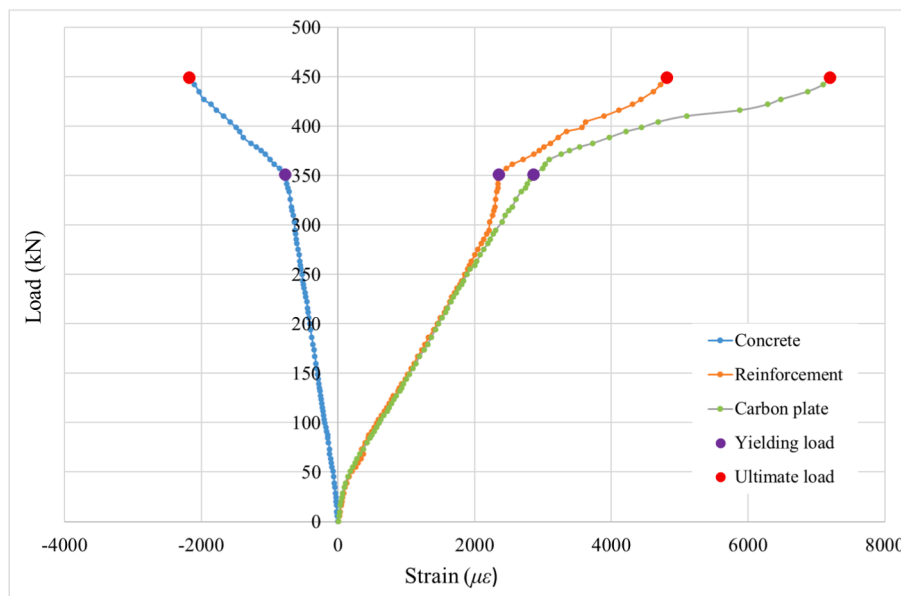
CRedit authorship contribution statement

Yu Deng: Conceptualization, Data curation, Formal analysis, Funding acquisition, Investigation, Methodology, Project administration, Resources, Supervision, Validation, Visualization, Writing – original draft, Writing – review & editing. **Zhen Guo:** Data curation, Formal analysis, Investigation, Methodology, Software, Validation, Visualization, Writing – original draft, Writing – review & editing. **Hexin Zhang:** Conceptualization, Data curation, Formal analysis, Funding acquisition,

Investigation, Methodology, Project administration, Resources, Supervision, Validation, Visualization, Writing – original draft, Writing – review & editing. **Suchart Limkatanyu:** Formal analysis, Investigation, Methodology, Validation, Writing – original draft, Writing – review & editing. **Piti Sukontasukkul:** Formal analysis, Investigation, Methodology, Validation, Writing – original draft, Writing – review & editing. **Terry Y.P. Yuen:** Formal analysis, Investigation, Methodology, Validation, Writing – original draft, Writing – review & editing. **Simon H.F. Wong:** Formal analysis, Methodology, Validation, Writing – original draft, Writing – review & editing. **Chayanon Hansapinyo:** Formal analysis, Methodology, Validation, Writing – original draft, Writing – review & editing. **Mark Adom-Asamoah:** Formal analysis, Methodology, Validation, Writing – original draft, Writing – review & editing. **Minhe Shen:** Formal analysis, Methodology, Validation, Writing – original draft, Writing – review & editing. **Longting Huang:** Validation, Writing – original draft, Writing – review & editing. **J.S. Kuang:** Investigation, Methodology, Validation, Writing – original draft, Writing



(g) SSL1A-3P



(h) SSL1B-4P

Fig. 10. (continued).

– review & editing. **Yiqing Zou:** Investigation, Resources, Writing – review & editing.

Declaration of Competing Interest

The authors declare that they have no known competing financial interests or personal relationships that could have appeared to influence the work reported in this paper.

Data availability

No data was used for the research described in the article.

Acknowledgements

This research was supported/partially supported by the National Nature Science Foundation of China (51768008, 52168016), British

Council and Ministry of Education, China (UK-China-BRI Countries Education Partnership Initiative 2019), British Council (Enabling Grants to Strengthen UK-China Institutional Partnerships through academic collaboration 2021), China Postdoctoral Science Foundation Project (2017M613273XB), Nature Science Foundation of Guangxi Zhuang Autonomous Region (2019JJA160137), Royal Academy of Engineering-Visiting Professor (VP2021\7\12), and Royal Academy of Engineering-Industrial Fellowship (IF\192023). The authors also would like to express their special gratitude for the support from Liuzhou OVM Machinery Co. Ltd., Liuzhou, Guangxi, China who provided the technical support on design, fabrication, and installation of the prestress components.

References

[1] [Shahawy M, Beitelman T. Flexural behavior of reinforced concrete beams strengthened with advanced composite materials. Covina, CA: Society for the Advancement of Material and Process Engineering; 1996.](#)

- [2] Deng Y, Li Z, Zhang H, Corigliano A, Lam ACC, Hansapinyo C, et al. Experimental and analytical investigation on flexural behaviour of RC beams strengthened with NSM CFRP prestressed concrete prisms. *Compos Struct* 2021;257:113385.
- [3] Deng Y, Ma F, Zhang H, Wong SHF, Pankaj P, Zhu L, et al. Experimental study on shear performance of RC beams strengthened with NSM CFRP prestressed concrete prisms. *Eng Struct* 2021;235:112004.
- [4] Deng Y, Shen M, Zhang H, Zhang P, Yuen TYP, Hansapinyo C, et al. Experimental and analytical studies on steel-reinforced concrete composite members with bonded prestressed CFRP tendon under eccentric tension. *Compos Struct* 2021;271:114124.
- [5] Deng Y, Gui J, Zhang H, Taliercio A, Zhang P, Wong SHF, et al. Study on crack width and crack resistance of eccentrically tensioned steel-reinforced concrete members prestressed by CFRP tendons. *Eng Struct* 2022;252:113651.
- [6] Haryanto Y, Hu H-T, Han Ay L, Hsiao F-P, Teng C-J, Hidayat Banu A, et al. Numerical investigation on RC T-beams strengthened in the negative moment region using NSM FRP rods at various depth of embedment. *Comput Concr* 2021;28:347–60.
- [7] Halder R, Yuen TYP, Chen W-W, Zhou X, Deb T, Zhang H, et al. Tendon stress evaluation of unbonded post-tensioned concrete segmental bridges with two-variable response surfaces. *Eng Struct* 2021;245:112984.
- [8] Zheng Y, Zhou N, Zhou L, Zhang H, Li H, Zhou Y. Experimental and theoretical study of bond behaviour between FRP bar and high-volume fly ash-self-compacting concrete. *Mater Struct* 2021;54:27.
- [9] Deng Y, Ling D, Guo Z, Sukontasukkul P, Yuen TYP, Wong SHF, et al. Strain driven mode-switching analytical framework for estimating flexural strength of RC box girders strengthened by prestressed CFRP plates with experimental validation. *Eng Struct* 2023;286:116084.
- [10] Wu ZS, Iwashita K, Hayashi K, Higuchi T, Murakami S, Koseki Y. Strengthening prestressed-concrete girders with externally prestressed PBO fiber reinforced polymer sheets. *J Reinf Plast Compos* 2003;22:1269–86.
- [11] Diab H, Wu Z, Iwashita K. Short and long-term bond performance of prestressed FRP sheet anchorages. *Eng Struct* 2009;31:1241–9.
- [12] Peng H, Zhang J, Shang S, Liu Y, Cai CS. Experimental study of flexural fatigue performance of reinforced concrete beams strengthened with prestressed CFRP plates. *Eng Struct* 2016;127:62–72.
- [13] Nader Tehrani B, Mostofinejad D, Hosseini SM. Experimental and analytical study on flexural strengthening of RC beams via prestressed EBROG CFRP plates. *Eng Struct* 2019;197:109395.
- [14] Deng J, Li X, Wang Y, Xie Y, Huang C. RC beams strengthened by prestressed CFRP plate subjected to sustained loading and continuous wetting condition: flexural behaviour. *Constr Build Mater* 2021;311:125290.
- [15] Deng J, Li J, Zhu M. Fatigue behavior of notched steel beams strengthened by a prestressed CFRP plate subjected to wetting/drying cycles. *Compos B Eng* 2022;230:109491.
- [16] Deng J, Li X, Zhu M, Ye Z. Fracture characteristics and stress transfer length of CFRP-concrete bond under field conditioning. *Int J Adhes Adhes* 2022;118:103231.
- [17] Deng J, Fei Z, Li J, Li H. Fatigue behaviour of notched steel beams strengthened by a self-prestressing SMA/CFRP composite. *Eng Struct* 2023;274:115077.
- [18] Zhu M, Li X, Deng J, Ye Z. Generalized evaluation of the effects of wet/dry cycling on CFRP-concrete bond subjected to low-cycle fatigue loading. *Eng Struct* 2022;269:114762.
- [19] Zhu M, Li X, Deng J, Ye Z, Li J. Bond degradation and EMI-based monitoring of CFRP to concrete interfaces exposed to wet-dry cycling. *Eng Struct* 2022;260:114225.
- [20] Li X, Zhu M, Liu Z, Deng J. EMI-based interfacial damage evolution of CFRP plates-strengthened RC beams under low-cycle fatigue loading and wetting/drying cycles. *Compos Struct* 2023;307:116653.
- [21] Li J, Xie Y, Zhu M, Xu H, Deng J. Degradation mechanism of steel/CFRP plate interface subjected to overloading fatigue and wetting/drying cycles. *Thin-Walled Struct* 2022;179:109644.
- [22] Tang W, Li S, Lu Y, Li Z. Combined effects of wetting–drying cycles and sustained load on the behaviour of FRP-strengthened RC beams. *Eng Struct* 2020;213:110570.
- [23] Yang D-S, Park S-K, Neale KW. Flexural behaviour of reinforced concrete beams strengthened with prestressed carbon composites. *Compos Struct* 2009;88:497–508.
- [24] Ahmed E, Sobuz HR, Sutan NM. Flexural performance of CFRP strengthened RC beams with different degrees of strengthening schemes. *Int J f Phys Sci* 2011;6:2229–38.
- [25] Weichen X, Yuan T, Xiaohui W. Calculation methods for flexural capacity of normal section of concrete beams prestressed with bonded FRP tendons [J]. *Build Struct* 2008;3.
- [26] Emdad R, Al-Mahaidi R. Effect of prestressed CFRP patches on crack growth of centre-notched steel plates. *Compos Struct* 2015;123:109–22.
- [27] Li Y, Wu Q, Yu Z, Liu Y. Destructive test study of the flexural load capacity of a full-scale reinforced concrete T-girder strengthened by externally prestressed CFRP plates. *Case Stud Constr Mater* 2022;16:e01035.
- [28] Chang X, Wang X, Liu C, Huang H, Zhu Z, Wu Z. Parametric analysis on the flexural behaviour of RC beams strengthened with prestressed FRP laminates. *Structures* 2023;47:105–20.
- [29] Zhelyazov T, Thorhallsson E. Numerical simulation of the behavior of the adhesive joint between FRP and concrete. In: Ilki A, Çavunt D, Çavunt YS, editors. *Building for the future: durable, sustainable, resilient*. Cham: Springer Nature Switzerland; 2023. p. 422–30.
- [30] Cornetti P, Muñoz-Reja M, Mantić V. Cohesive Crack Models and Finite Fracture Mechanics analytical solutions for FRP-concrete single-lap shear test: an overview. *Thin Appl Fract Mech* 2022;122:103529.
- [31] Jin L, Chen H, Wang Z, Du X. Size effect on axial compressive failure of CFRP-wrapped square concrete columns: tests and simulations. *Compos Struct* 2020;254:112843.
- [32] Heydarinouri H, Motavalli M, Nussbaumer A, Ghafouri E. Development of mechanical strengthening system for bridge connections using prestressed CFRP rods. *J Struct Eng* 2021;147:04020351.
- [33] Grace NF, Singh S, Shinouda MM, Mathew SS. Flexural response of CFRP prestressed concrete box beams for highway bridges. *PCI J* 2004;49.
- [34] Grace Nabil F, Jensen Elin A, Noamesi DK. Flexural performance of carbon fiber-reinforced polymer prestressed concrete side-by-side box beam bridge. *J Compos Constr* 2011;15:663–71.
- [35] Grace NF, Enomoto T, Sachidanandan S, Puravankara S. Use of CFRP/CFCC reinforcement in prestressed concrete box-beam bridges. *ACI Struct J* 2006;103:123–32.
- [36] Shang S, Peng H, Tong H, Wei D, Zeng L. Study of strengthening reinforced concrete beam using prestressed carbon fiber sheet. *J Build Struct* 2003;24:24–30.